



Comparison of GERB instantaneous radiance and flux products with CERES Edition-2 data

N. Clerbaux^{a,*}, J.E. Russell^b, S. Dewitte^a, C. Bertrand^a, D. Caprion^a, B. De Paepe^a, L. Gonzalez Sotelino^a, A. Ipe^a, R. Bantges^b, H.E. Brindley^b

^a Royal Meteorological Institute of Belgium, Belgium

^b Imperial College, London, United Kingdom

ARTICLE INFO

Article history:

Received 25 April 2008

Received in revised form 22 August 2008

Accepted 24 August 2008

Keywords:

Earth radiation Budget

GERB

SEVIRI

CERES

ABSTRACT

Whenever possible, intercomparisons of Earth radiation budget data from different spaceborne instruments should be made as they are important steps in the overall validation process. Intercomparisons are also key elements to compile long-term climate datasets by merging data from several instruments. In this study the GERB Edition-1 and CERES Edition-2 data are compared for June and December 2004. The comparisons concern shortwave and longwave radiance and flux at the top-of-atmosphere. Three different GERB level-2 data products with differing space–time characteristics are compared with data from the 4 CERES instruments. In general, the GERB unfiltered radiances and fluxes are found to be 5.9% and 7.5% higher than CERES for the shortwave. The GERB longwave radiance and flux are 1.3% lower than CERES. Analysis separated by scene type reveals differences between the GERB products. These differences should be taken into account by the user of the GERB data. The LW flux intercomparison shows angular dependency problem affecting the GERB dataset in cloudy and aerosol regions.

© 2008 Elsevier Inc. All rights reserved.

1. Introduction

The Geostationary Earth Radiation Budget (GERB, Harries et al., 2005) instruments are the first BroadBand (BB) radiometers designed to operate from geostationary orbit. They are part of the Meteosat Second Generation (MSG, Schmets et al., 2002) satellites payload and have as a main objective the accurate observation of the diurnal cycle of the Earth radiation budget at the Top-Of-Atmosphere (TOA). The first GERB instrument (identified as GERB-2 for historical reasons) was launched on Meteosat-8 in 2002 and provided operational BB observations from March 26th 2004 to May 10th 2007. Since then the GERB operational service is provided by the GERB-1 instrument on Meteosat-9, while GERB-2 is activated on a regular basis for GERB instrument intercomparison.

The ground processing of the GERB data is distributed between the United Kingdom and Belgium. The Rutherford Appleton Laboratory (RAL, UK) is responsible for the calibration and the geolocation of the instrument's measurements. This generates geolocated filtered radiances which are transferred to the Royal Meteorological Institute of Belgium (RMIB) where the radiances are unfiltered and converted into fluxes (see Dewitte et al., 2008 for an overview of the GERB data

processing at RMIB). The resulting GERB level-2 products are provided to the user community in three formats: ARG, BARG and HR (see definitions in the next section), which differ in their spatial and temporal properties. The GERB-2 ARG data has been released for scientific use as Edition-1 while the similar data in the BARG and HR formats are still under validation. This work is a step in the validation process of the BARG and HR products.

In this study, the shortwave (SW) and longwave (LW) TOA radiances and fluxes of the GERB-2 instrument are compared with the corresponding quantities provided by the Clouds and Earth's Radiant Energy System (CERES, Wielicki et al., 1996) instruments on the polar orbiting Terra and Aqua NASA satellites. Following previous works of Haefelin et al. (2001), the comparisons are done on temporally and spatially collocated measurements, with an additional coangularity criteria for the radiance comparisons.

The aimed absolute accuracy of the GERB products is 1% at 1 Standard Deviation (SD) for both the unfiltered SW and LW radiances. However, the theoretical accuracy of the Edition 1 GERB products does not meet this target for the SW channel. The sources of uncertainty are (Russell, 2006): the absolute calibration (SW=0.22% and LW=0.05% at 1 SD), spectral response characterization (SW=1.9% and LW=0.9% at 1SD), and unfiltering process (SW=0.56% and LW=0.06% at 1 SD). A root mean square sum of these errors leads to uncertainties at 1 SD of 1.99% (SW) and 0.9% (LW). In both cases, the main source of the uncertainty is the characterization of the GERB spectral sensitivity. It is worth noting that there are ongoing studies relating to the ground

* Corresponding author. Royal Meteorological Institute of Belgium, Department of Observations, Section Remote Sensing from Space, Building B, Avenue Circulaire 3, 1180 Brussels, Belgium.

E-mail address: Nicolas.Clerbaux@oma.be (N. Clerbaux).

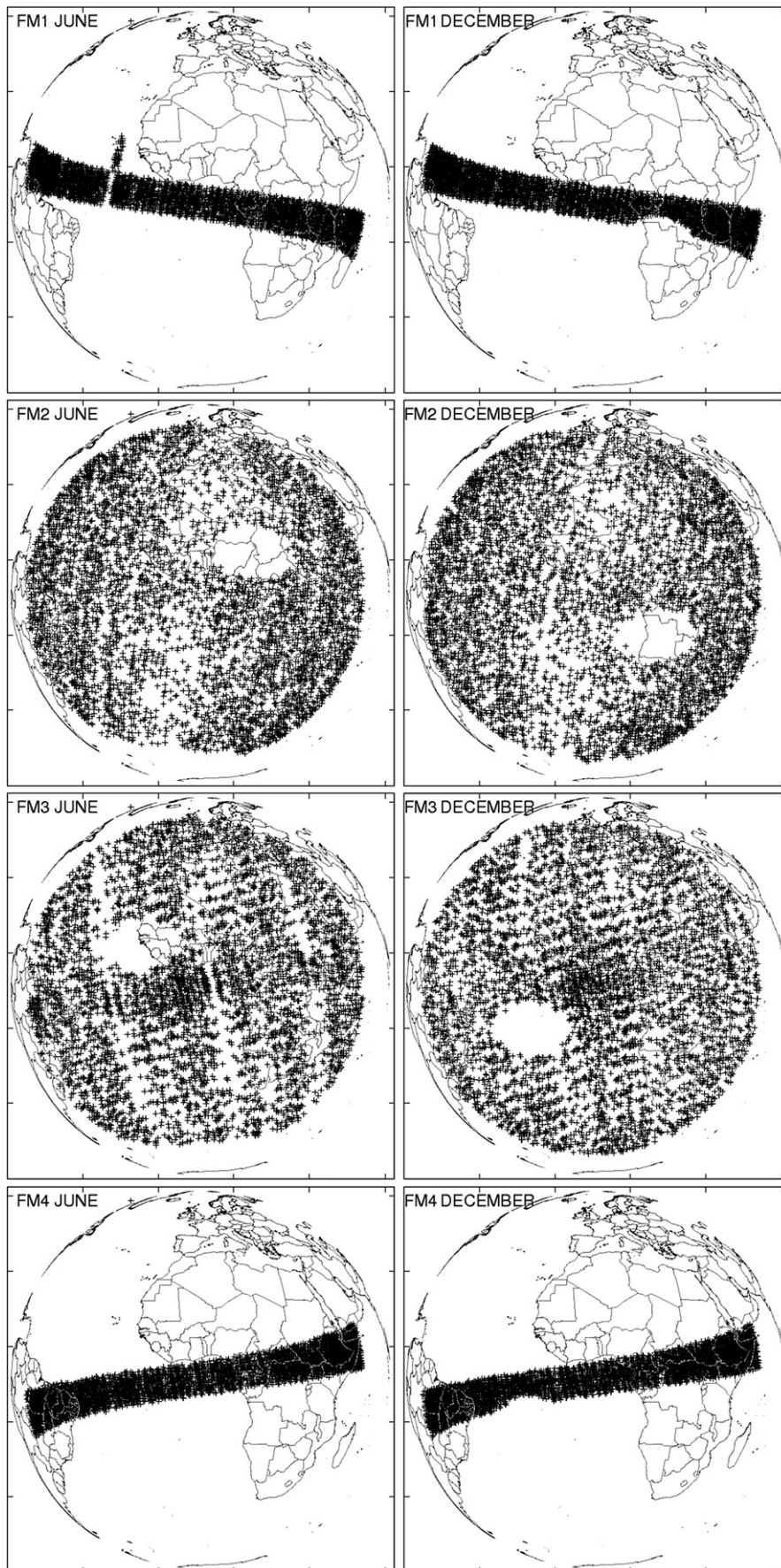


Fig. 1. Positions of the daytime GERB/CERES coangular observations ($\alpha < 5^\circ$) for the FM1, FM2, FM3, FM4 in June and December 2004 (subsets of 5000 points are shown for clearness). During the night there is no more sun-glint area and the patterns are inverted (FM1 looks like FM4 and vice versa).

Table 1
Numbers of coangular radiance pairs and collocated flux pairs for the SW (top) and LW radiation (bottom)

	$\alpha < 2^\circ$			$\alpha < 5^\circ$			$\alpha < 8^\circ$			Flux		
	ARG	BARG	HR	ARG	BARG	HR	ARG	BARG	HR	ARG	BARG	HR
<i>Number of shortwave observation pairs</i>												
FM1	4311	4085	8065	19,677	18,486	48,801	45,498	42,563	122,336	2,488,934	2,351,097	10,876,945
FM2	74,378	70,860	178,231	147,785	139,949	478,060	218,491	20,6734	768,378	2,514,313	2,392,723	14,839,086
FM3	6767	6640	7835	32,176	31,308	47,029	74,553	72,201	120,409	2,378,288	2,328,791	11,852,073
FM4	4369	4145	8093	20,125	18,906	49,042	46,533	43,908	124,137	2,499,618	2,401,754	11,008,608
<i>Number of longwave observation pairs</i>												
FM1	11,478	8267	16,374	53,326	38,177	98,975	123,889	88,665	250,902	7,140,077	5,154,527	23,544,997
FM2	112,533	81,116	201,756	240,593	172,238	577,490	378,152	270,975	985,685	7,422,034	5,407,764	32,057,576
FM3	18,596	13,845	15,903	88,230	65,589	96,321	203,982	150,750	247,574	6,540,438	4,960,310	25,242,110
FM4	11,794	8420	16,310	53,923	38,739	100,255	125,384	90,237	254,416	7,108,241	5,161,206	23,581,383

characterization of the GERB-2 spectral response which may result in changes to this parameter for the GERB Edition-2 processing. This could modify the absolute level of the GERB SW channel.

Concerning the CERES radiances, the required absolute accuracy at 1 SD is 1% for the SW and 0.5% for the LW (Wielicki et al., 1996). Recently, Loeb et al. (in press) performed a detailed analysis of the uncertainty of the CERES measurements. They evaluate at 1% and 0.75% the accuracies of the SW and LW channels at 1 SD. An Edition-3 of the CERES datasets is in preparation. This edition would correct for observed darkening of the SW quartz filter more completely than addressed by the Edition-2 Rev1 used in this study.

Section 2 presents the data used for this study and describes the ARG, BARG and HR GERB data format. Section 3 describes the methodology for the GERB/CERES matching and statistical analysis. Sections 4–7 show the comparison results for the SW radiances, SW fluxes, LW radiances, and LW fluxes, respectively. Section 8 summarizes the results obtained and provides recommendations to the GERB data users.

2. Data used

2.1. Intercomparison periods

GERB/CERES comparisons have been made for the months of June and December 2004. As well as providing maximum difference in solar illumination, these months embrace two special observation campaigns when the CERES Flight Model-2 (FM2) instrument was operated in a special scanning mode that optimizes the frequency of coangular observations with GERB (Smith et al., 2003). During these campaigns the azimuth of the scanning plane of CERES is oriented parallel to the GERB line-of-sight. As these campaigns extended into the beginning of the following months, the 1st to 10th of July 2004 and January 2005 have been added to the June and December periods for the FM2 radiance comparisons in Section 4. All the other comparisons are based on the 30 days of June 2004 and the 31 days of December 2004.

2.2. GERB data

The GERB level-2 data provide TOA unfiltered radiance and flux for both the SW and LW. In this work, SW and LW do not refer to wavelength ranges but instead to the type of radiation: SW is used for reflected solar radiation while LW for emitted thermal radiation. The level-2 data are available in 3 formats that differ in the spatial and temporal processing applied to the GERB observations. The original observations are made over a Point Spread Function (PSF) with a full-width half maximum of 68 km East–West \times 38 km North–South at satellite nadir. The wings of the PSF extend much further (e.g. 140 \times 71 km for the full-width at the 10% sensitivity level). Despite significant effort to improve this part of the processing, the current 1 standard deviation noise on the geolocation of these observations is a quarter of GERB pixel (the target accuracy is 0.1 pixel). Although the

geolocation of the GERB footprint changes for each scan, the level-2 data are presented on fixed rectified grids. The three level-2 data products are presented on different grids and therefore undergo different rectification processes, as described in Dewitte et al. (2008) and summarized hereafter.

The Averaged Rectified and Geolocated (ARG) data are an average of three successive GERB scans (covering a period of approximately 17 min) presented on a regular (in viewing angle) grid with a sampling distance of 44 \times 44 km at nadir. The ARG values are obtained by bilinear interpolation of the original observations. As no attempt is made to correct for the GERB PSF the radiance and flux values at each grid point are representative of the energy from a larger region than the grid spacing. Additionally the GERB geolocation noise and the linear interpolation of the observations will affect the radiance and flux values at each point.

The Binned Averaged Rectified and Geolocated (BARG) products are averages over fixed 15 minute time intervals (00:00 to 00:15 UTC, 00:15 to 00:30 UTC, etc.) presented on a regular (in viewing angle) grid with a spacing of 45 \times 45 km at nadir. The processing is considerably more complex than for the production of the ARG. It attempts to remove the effect of the PSF, and also provides corrections for errors that may have been introduced in the ARG by the geolocation and rectification processes. This is achieved by using fine scale estimates of the broadband SW and LW radiances inferred from narrowband measurements made by the Spinning Enhanced Visible and Infrared Radiometer Imager (SEVIRI, Schmetz et al., 2002) instrument on the same MSG satellite. The SEVIRI narrowband-to-broadband estimation is described in Clerbaux et al. (2005). Merging the GERB BB observations and the fine scale SEVIRI BB estimates results in level-2 BARG radiances and fluxes which are representative of the radiation from exact 15 \times 15 SEVIRI pixel areas (i.e. 45 km).

Finally, the High Resolution (HR) product is presented on a grid with a spacing of 3 \times 3 SEVIRI pixels (i.e. 9 \times 9 km at nadir). It is provided every 15 min as instantaneous values at the time of the SEVIRI observations. As for the BARG, fine scale estimates of the BB radiances from SEVIRI are combined with GERB observations to produce the GERB High Resolution data. The GERB HR product allows the study of the radiation budget at relatively small scales (e.g. valley fog).

The current state-of-the-art version of the GERB-2 data is the ‘Version-3’ (V003). After validation and manual quality checks, the Version-3 is labeled ‘Edition-1’ and is put in the GERB archive. Currently validated Edition-1 data only exist for the ARG format. However, Version-3 BARG and HR data have been made available for validation activities in anticipation of their future release. As part of this process, the Edition-1 ARG and Version-3 BARG and HR GERB data are compared with CERES in this work.

2.3. CERES data

For CERES we used the instantaneous TOA radiances and fluxes which are available in the Edition-2 of the ‘Single Scanner Footprint

Table 2
GERB/CERES SW radiance ratio m and uncertainty for $\alpha < 5^\circ$

Scene type	FM1	FM2	FM3	FM4	<FM>	< L_g >	ΔL
<i>Averaged Rectified Geolocated (ARG)</i>							
Allsky	1.044±0.005	1.054±0.004	1.072±0.004	1.068±0.005	1.059	76.25	4.21
June	1.042±0.008	1.058±0.006	1.073±0.006	1.070±0.007	1.061	70.92	4.02
December	1.046±0.008	1.051±0.006	1.070±0.005	1.066±0.008	1.058	81.46	4.39
Overcast	1.008±0.010	1.026±0.008	1.035±0.009	1.023±0.018	1.023	177.11	3.70
Clearsky	1.077±0.019	1.066±0.004	1.088±0.004	1.097±0.017	1.082	62.06	4.58
Ocean	1.120±0.087	1.143±0.025	1.093±0.024	1.076±0.046	1.108	25.70	2.49
Dark veg.	1.071±0.020	1.077±0.006	1.098±0.015	1.104±0.018	1.088	50.24	4.03
Bright veg.	1.067±0.011	1.063±0.005	1.086±0.008	1.105±0.016	1.080	56.61	4.17
Dark desert	–	1.078±0.009	1.083±0.023	–	1.081	77.73	5.78
Bright desert	–	1.060±0.004	1.086±0.007	–	1.073	114.18	7.78
<i>Binned Averaged Rectified Geolocated (BARG)</i>							
Allsky	1.045±0.004	1.054±0.003	1.071±0.004	1.067±0.004	1.059	76.51	4.24
June	1.044±0.006	1.057±0.004	1.074±0.007	1.068±0.005	1.061	71.28	4.08
December	1.045±0.006	1.052±0.005	1.068±0.004	1.066±0.005	1.058	81.62	4.40
Overcast	1.041±0.008	1.050±0.005	1.062±0.007	1.064±0.014	1.054	181.28	9.28
Clearsky	1.065±0.012	1.065±0.003	1.087±0.004	1.078±0.014	1.074	55.38	3.88
Ocean	1.055±0.024	1.084±0.010	1.067±0.013	1.038±0.019	1.061	24.00	1.33
Dark veg.	1.073±0.010	1.072±0.005	1.091±0.008	1.099±0.015	1.084	50.14	3.86
Bright veg.	1.070±0.014	1.062±0.005	1.086±0.009	1.105±0.014	1.081	56.81	4.24
Dark desert	–	1.062±0.007	1.088±0.011	1.080±0.031	1.077	82.13	5.90
Bright desert	–	1.066±0.002	1.093±0.004	–	1.079	114.34	8.40
<i>High Resolution (HR)</i>							
Allsky	1.046±0.003	1.057±0.003	1.071±0.003	1.067±0.003	1.060	74.23	4.17
June	1.045±0.004	1.060±0.005	1.073±0.004	1.069±0.003	1.062	69.25	4.04
December	1.047±0.005	1.054±0.002	1.068±0.004	1.064±0.004	1.058	79.03	4.30
Overcast	1.033±0.008	1.053±0.005	1.061±0.006	1.054±0.008	1.050	171.45	8.05
Clearsky	1.064±0.012	1.066±0.004	1.088±0.004	1.067±0.016	1.071	52.92	3.65
Ocean	1.054±0.019	1.081±0.011	1.066±0.013	1.054±0.025	1.064	24.53	1.43
Dark veg.	1.080±0.016	1.072±0.005	1.095±0.008	1.096±0.011	1.086	51.65	4.07
Bright veg.	1.069±0.015	1.065±0.005	1.086±0.006	1.098±0.011	1.079	56.83	4.12
Dark desert	–	1.063±0.006	1.091±0.010	1.078±0.013	1.077	79.01	5.69
Bright desert	–	1.067±0.002	1.098±0.005	–	1.082	113.82	8.59

The last columns give the average GERB radiance $\langle L_g \rangle$ and the difference in average radiance $\Delta L = \langle L_g \rangle - \langle L_c \rangle$ both in $W\ m^{-2}\ sr^{-1}$.

TOA/Surface Fluxes and Clouds” (SSF) product. The correction for the SW quartz filter darkening has been performed as recommended by the CERES team to obtain the “Revision-1” data. For the clear ocean CERES footprints, the specific Revision-1 correction is applied. So, CERES SSF Edition-2/Rev1 are used for these intercomparisons.

During June and December 2004 the CERES FM1 and FM4 instruments were operated in cross-track mode while the FM2 and FM3 instruments were mainly operated in Rotating Azimuth Plane Scan (RAPS) modes. As already stated, the FM2 instrument has been operated in Programmable Azimuth Plane Scan (PAPS) mode during some orbits to maximize the number of coangular observations with GERB.

FM1 and FM2 are on the sun-synchronous Terra satellite providing measurements close to 10:30 and 22:30 local time. FM3 and FM4 are on the sister Aqua satellite and provide measurements close to 13:30 and 01:30. Therefore GERB/CERES LW comparisons concentrate over 4 clusters of local time and the SW over the 2 daytime clusters.

For the flux intercomparison, a scaling factor of $(r_e + 20\ km)^2 / r_e^2 = 1.00629$, where r_e is the Earth Equatorial radius, is applied to the CERES SSF fluxes to scale them from the 20 km reference level used for the CERES SSF TOA fluxes (Loeb et al., 2002) to the surface reference level used for GERB.

3. Methodology

3.1. Collocation methodology

In a first step, databases of corresponding GERB and CERES observations are built by spatial average of the observations of one instrument in the footprint of the second instrument. The choice is made according to the respective size of the CERES footprints (20 km

at nadir) and GERB level-2 pixel size (44 km for ARG, 45 km for BARG and 9 km for HR).

For the ARG and the BARG formats, the CERES observations that fall within each pixel are averaged. For the HR, the opposite is done: the GERB HR values that fall within the CERES PSF are averaged. In this case, the CERES PSF in the HR grid is modeled as a disk with radius of $(20\ km / \cos(VZA_{ceres})) / (9\ km / \cos(VZA_{gerb}))$ HR pixel. It is known that there is no correction for the PSF in the ARG format and thus the ARG radiance at each grid point will contain contributions from regions outside the grid spacing. This paper attempts to quantify the error introduced by treating this product as a representation of a uniform average of the radiance and flux within each grid point as it is expected that this will be how it is primarily employed.

Concerning the temporal matching, only the CERES observations that fall within the ARG and BARG averaging periods (17 and 15 min respectively) are considered. Sensitivity studies have demonstrated that the results of the comparison do not depend on the temporal matching criteria. For the matching with the instantaneous HR product, a maximum difference of 5 min is allowed for the CERES observations.

This collocation methodology is applied to the radiance and flux and as described below also on the cloud fraction, the cloud optical depth, and the viewing angles.

3.2. Coangularity criteria

For the radiance comparisons, observations which are not ‘coangular’ are rejected before being averaged. For this, a threshold value is applied on the angle α between the GERB and CERES directions of observation. Databases of coangular radiances have been extracted using different values for the threshold value: $\alpha < 2^\circ$, $\alpha < 5^\circ$, and $\alpha < 8^\circ$. Strict coangularity

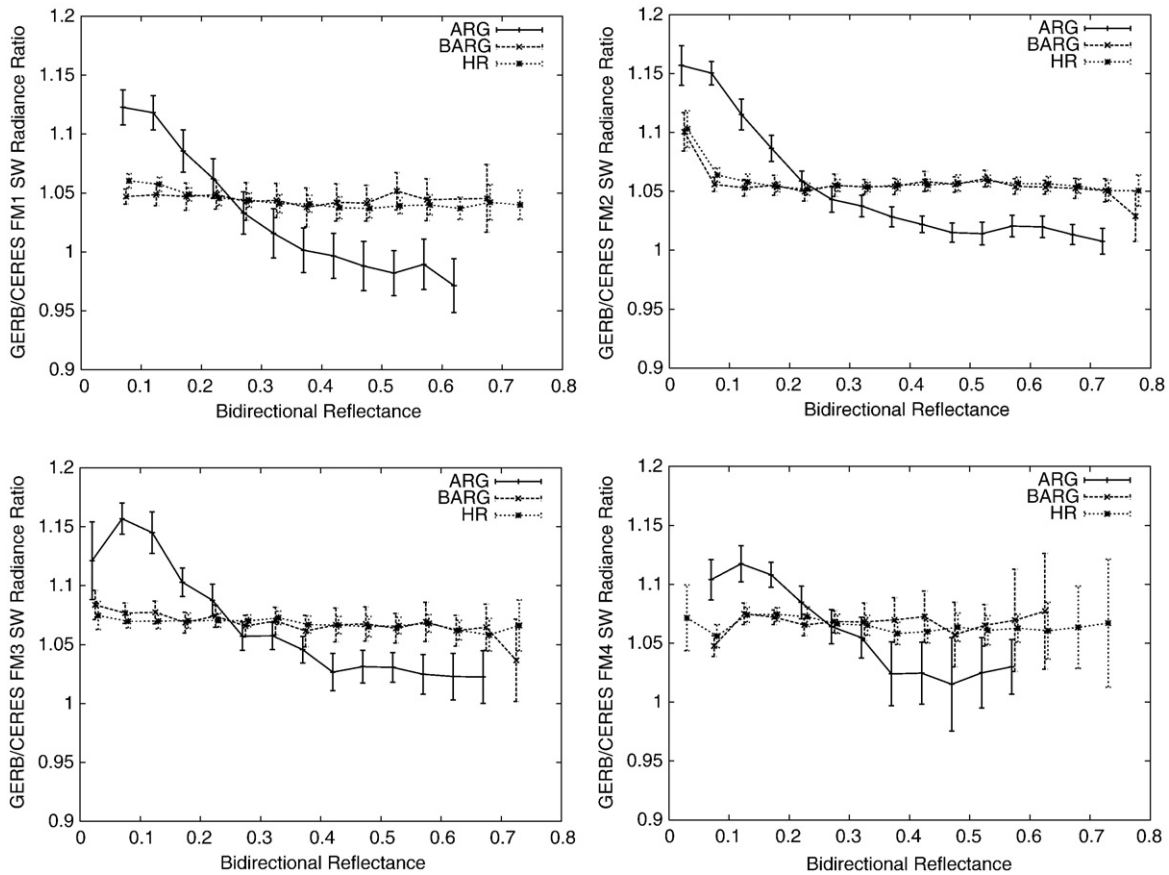


Fig. 2. GERB/CERES SW radiance ratio m and uncertainty in reflectance bins for $\alpha < 5^\circ$.

criteria is desirable to improve the radiance matching for highly anisotropic scenes but on the other hand provides poorer statistic. The radiance comparisons presented in this work are mostly based on the $\alpha < 5^\circ$ coangularity criteria. However, the 2° and 8° criteria have been used to demonstrate that the comparison results are not sensitive to the chosen threshold value.

Fig. 1 shows the location of the GERB/CERES coangular observations in June and December 2004. Coverage of the full GERB field of view is only possible with CERES instrument in RAPS or PAPS mode. Coangular observations for CERES instruments in cross-track mode (FM1 and FM4) are restricted to the tropical belt.

Table 1 gives the numbers of observation pairs for the different CERES instruments, the 3 GERB data formats, and the 2° , 5° , and 8° thresholds for α . The value of the special scanning mode used for the FM2 during the GERB campaigns is obvious, especially when strict coangularity criteria is used ($\alpha < 2^\circ$). The last columns of the table provide the statistics without any coangularity criteria, indicating the matches for the flux comparisons.

3.3. Cloud type dependency

Fraction of cloud cover and mean cloud optical depth τ at $0.6 \mu\text{m}$ are available in the GERB level-2 data (ARG, BARG, and HR) as well as in the CERES SSF files. These quantities are averaged during the collocation processing in a similar way as the radiance and flux (the smaller pixels are averaged up to the bigger pixels). To address scene type dependency that may affect the GERB/CERES comparisons, these cloud retrievals are combined as follows. A matched GERB/CERES observation pair is said “clear” if both GERB and CERES data have cloud fraction of 0%. A pair is said “overcast” if both data

have cloud fraction of 100% and cloud optical depth higher than 7.39.

The GERB cloud fraction and optical depth are based on the SEVIRI solar channels (Ipe et al., submitted for publication) and are therefore not available during night time. For this reason, the cloud type dependency for the LW comparison is only based on the CERES cloud information. For the clear scenes, separate comparisons are made according to the surface type provided in the GERB files.

3.4. Statistical analysis

Intercomparisons of radiometric instruments can be expressed as differences (e.g. in $\text{W m}^{-2} \text{sr}^{-1}$) or as ratios (unitless). As the GERB/CERES scatterplots indicate that most of the disparity is explained by multiplicative factors, the second option is adopted in this paper.

The ratio of the average GERB and CERES quantities is estimated on a daily basis

$$m_{\text{day}} = \frac{\langle \nu_{\text{gerb}} \rangle}{\langle \nu_{\text{ceres}} \rangle} \quad (1)$$

where the quantity ν can be SW or LW radiance or flux. The daily basis is adopted because this time period is the time needed by a CERES instrument to scan all the Meteosat FOV. Therefore the daily m_{day} values are expected to be stable day after day, even if there exist regional patterns in the GERB/CERES ratio. The daily value m_{day} is estimated only if the number of GERB/CERES observation pairs is higher than 5. This number is always reached in allsky conditions but may not be reached for radiance comparison in some restrictive conditions.

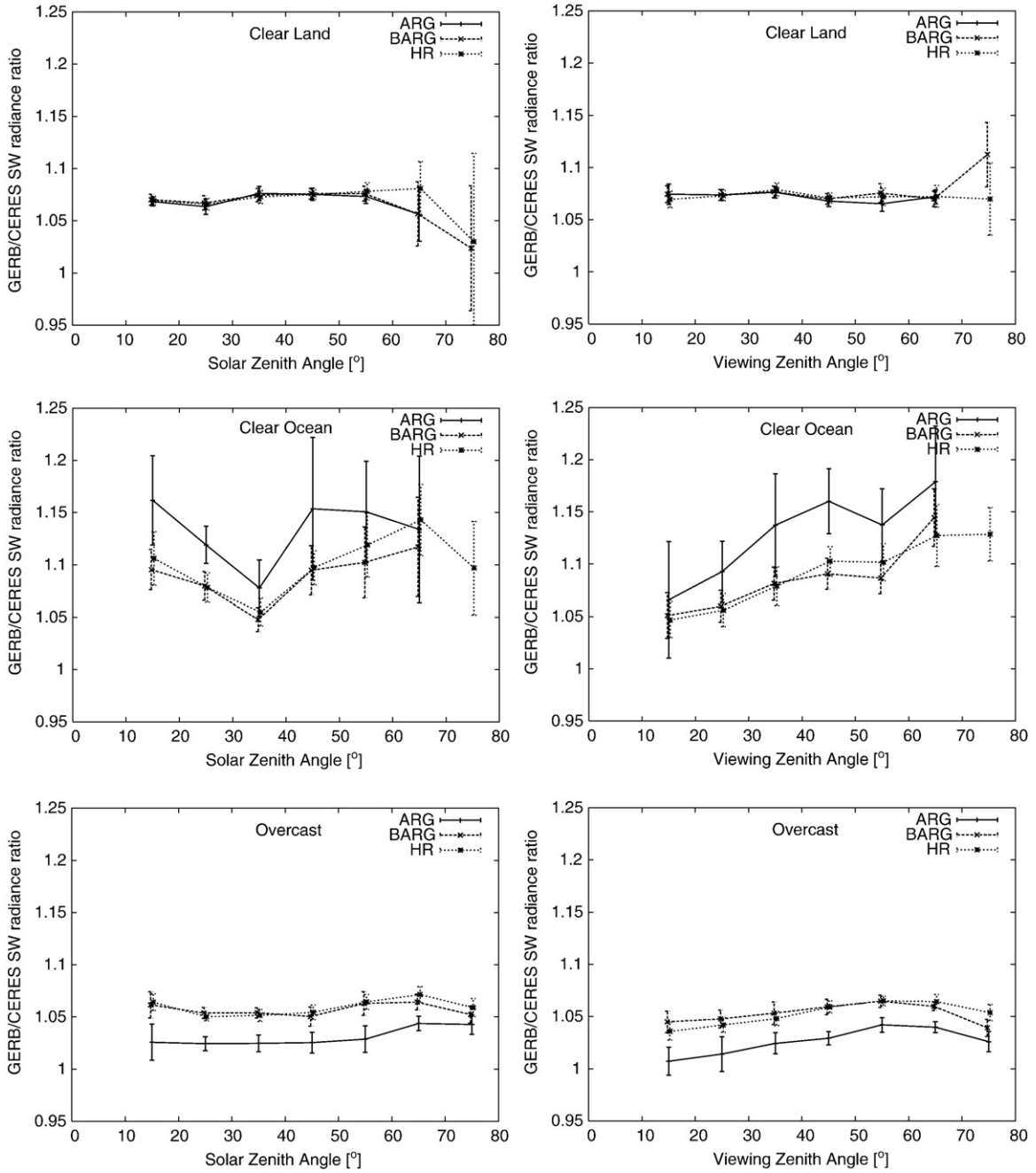


Fig. 3. Angular dependencies of the GERB/CERES SW radiance ratio m with the Solar Zenith Angle (SZA, left) and the Viewing Zenith Angle (VZA, right). Top, middle and bottom graphs are for clear land, clear ocean and overcast, respectively.

Let N be the number of daily ratio values, the best estimate of the GERB/CERES ratio m and the associated uncertainty are

$$m = \mu(m_{\text{day}}) \pm \frac{3\sigma(m_{\text{day}})}{\sqrt{N-1}} \quad (2)$$

where

$$\mu(m_{\text{day}}) = \frac{1}{N} \sum_{\text{day}=1}^N m_{\text{day}} \quad (3)$$

$$\sigma(m_{\text{day}}) = \sqrt{\frac{1}{N} \sum_{\text{day}=1}^N (m_{\text{day}} - \mu(m_{\text{day}}))^2} \quad (4)$$

are the mean and standard deviation of the daily values. The factor 3 in Eq. (2) is used to have a likelihood of greater than 99% (assuming a normal distribution of the m_{day}). It is worth considering that GERB/CERES ratios

observed over very dark (SW) or cold (LW) scenes correspond to small absolute differences and will then vanish in the averaging process. For this reason, the average GERB radiance $\langle L_{\text{gerb}} \rangle$ or flux $\langle F_{\text{gerb}} \rangle$ are provided in addition to the average ratio and uncertainty to allow conversion of the ratio m to an absolute difference.

3.5. Regional analysis

Regional analysis is performed by averaging the GERB and CERES values within $N \times N$ BARG pixel regions and ratioing the resulting values. For the radiance comparison $N=10$ (i.e. 450 km size at nadir) are used. For the flux comparison the value $N=7$ and $N=4$ are used for the SW and LW radiation, respectively. The regional analysis is performed for allsky and for clearsky conditions. Here clearsky is defined

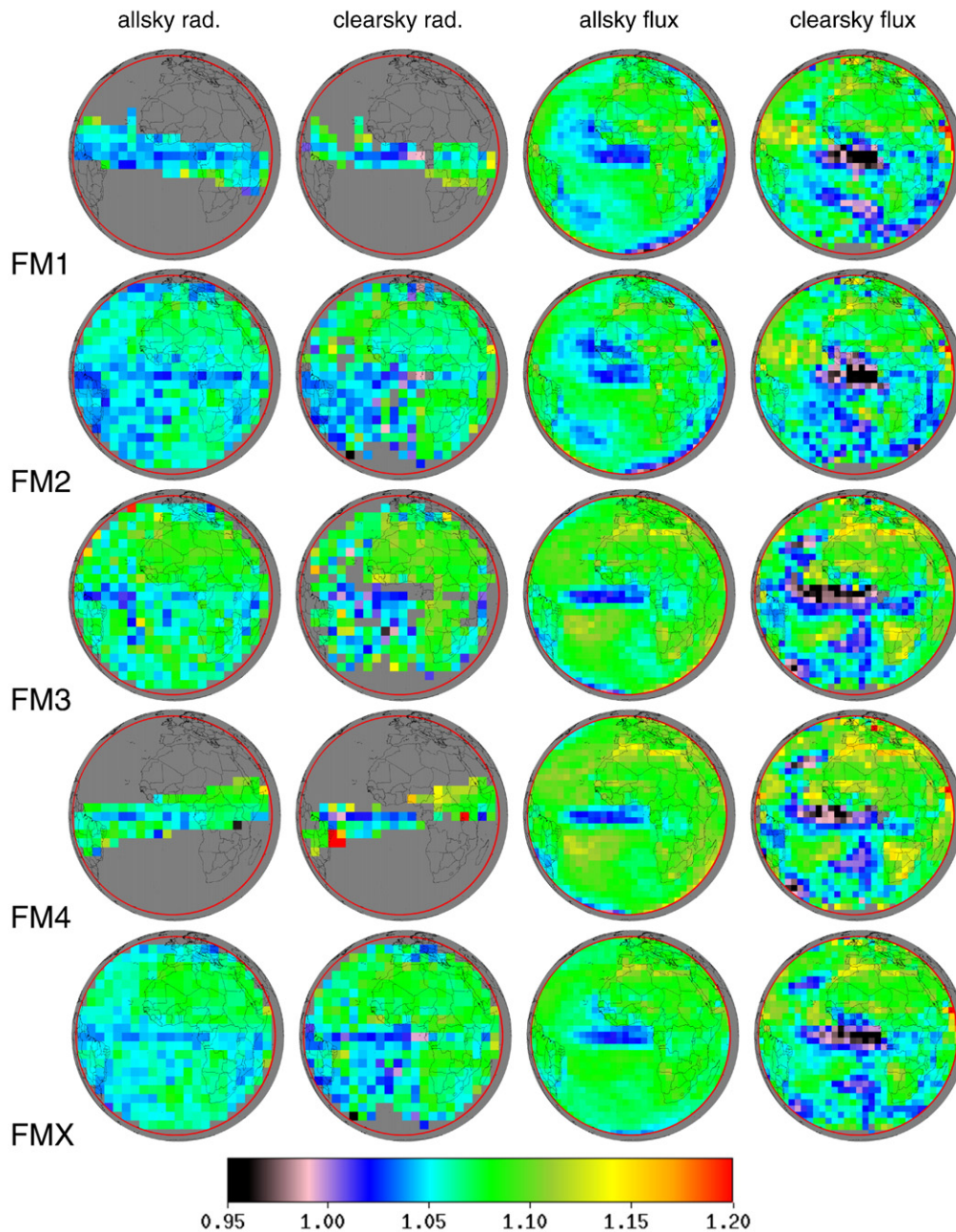


Fig. 4. GERB (BARG)/CERES SW ratio for the different CERES instruments and all together (FMX). The red circle indicates VZA = 70°.

as cloud fractions lower than 10% for both GERB and CERES observations. Note: 10% is used rather than 0% to provide sufficient numbers of clear data in most of the boxes. It was however demonstrated that the results are not significantly affected by 10% threshold. If the number of observation pairs in a box is lower than 20, the box appears in grey on the regional comparison images. For the regional comparison of the coangular radiance the criteria $\alpha < 8^\circ$ is used to have a better statistics in each box.

4. Shortwave radiance comparison

Table 2 provides the shortwave radiance comparison results for the $\alpha < 5^\circ$ criteria (similar results, not shown, are obtained with the $\alpha < 2^\circ$ and $\alpha < 8^\circ$ criteria). As the CERES VZA is limited to about 63° due to the needed coverage with the Moderate Resolution Imaging Spectro-

radiometer (MODIS) imager, the statistical analysis considers only the GERB observations with VZA $< 60^\circ$. In all the comparisons (for all GERB formats, all CERES instruments, and scene types) the GERB SW radiance is higher than CERES. In allsky conditions the GERB/CERES ratio m does not depend significantly (wrt the uncertainty on m) on the GERB format but instead exhibits significant differences with the different CERES instruments: $m = 1.045$ for FM1, $m = 1.054$ for FM2, $m = 1.072$ for FM3, and $m = 1.068$ for FM4. A straight average of the ratio for the 4 CERES instruments (column <FM> in the table) indicates that the GERB SW radiance is 5.9% higher than CERES. The ratios for June and December are in good agreement with a (non-significant) difference of about 0.003.

Scene type dependency is observed by the variation of m for overcast and clear conditions over various surfaces. Here significant differences are observed between the GERB ARG format on one side

Table 3
GERB/CERES SW flux ratio m and uncertainty

Scene type	FM1	FM2	FM3	FM4	<FM>	< F_g >	ΔF
<i>Averaged Rectified Geolocated (ARG)</i>							
Allsky	1.066±0.002	1.066±0.002	1.079±0.001	1.085±0.001	1.074	253.22	17.44
June	1.068±0.002	1.069±0.002	1.078±0.002	1.086±0.002	1.075	233.73	16.34
December	1.065±0.002	1.063±0.002	1.080±0.002	1.084±0.002	1.073	272.13	18.50
Overcast	1.038±0.003	1.043±0.003	1.056±0.003	1.056±0.003	1.048	493.24	22.52
Clearsky	1.077±0.003	1.074±0.002	1.096±0.003	1.099±0.002	1.086	262.34	20.84
Ocean	1.081±0.014	1.093±0.012	1.090±0.012	1.085±0.013	1.087	94.06	7.54
Dark veg.	1.071±0.004	1.069±0.004	1.085±0.007	1.095±0.006	1.080	160.25	11.83
Bright veg.	1.084±0.004	1.078±0.004	1.111±0.007	1.118±0.006	1.098	197.87	17.52
Dark desert	1.091±0.004	1.084±0.004	1.108±0.006	1.114±0.005	1.099	240.54	21.60
Bright desert	1.072±0.003	1.070±0.003	1.091±0.003	1.093±0.003	1.082	356.88	26.80
<i>Binned Averaged Rectified Geolocated (BARG)</i>							
Allsky	1.066±0.002	1.066±0.002	1.080±0.002	1.086±0.001	1.075	253.98	17.59
June	1.067±0.002	1.069±0.002	1.080±0.003	1.087±0.002	1.076	234.58	16.51
December	1.065±0.002	1.063±0.002	1.081±0.002	1.085±0.002	1.073	272.69	18.64
Overcast	1.059±0.002	1.066±0.003	1.079±0.002	1.080±0.002	1.071	506.21	33.36
Clearsky	1.076±0.002	1.073±0.002	1.096±0.002	1.098±0.002	1.085	246.67	19.41
Ocean	1.046±0.009	1.058±0.008	1.063±0.009	1.057±0.008	1.056	91.26	4.83
Dark veg.	1.071±0.005	1.068±0.005	1.082±0.006	1.092±0.006	1.078	160.67	11.58
Bright veg.	1.083±0.004	1.077±0.004	1.113±0.007	1.120±0.006	1.098	195.42	17.30
Dark desert	1.070±0.004	1.066±0.005	1.083±0.004	1.088±0.003	1.076	235.00	16.58
Bright desert	1.078±0.003	1.076±0.002	1.098±0.003	1.100±0.003	1.088	357.18	28.71
<i>High Resolution (HR)</i>							
Allsky	1.067±0.002	1.066±0.002	1.082±0.002	1.086±0.002	1.075	253.65	17.65
June	1.069±0.002	1.069±0.002	1.082±0.003	1.088±0.003	1.077	231.39	16.50
December	1.065±0.003	1.064±0.002	1.081±0.002	1.084±0.002	1.073	275.22	18.76
Overcast	1.055±0.003	1.062±0.003	1.078±0.003	1.077±0.003	1.068	481.40	30.54
Clearsky	1.077±0.002	1.075±0.002	1.096±0.003	1.097±0.003	1.086	231.32	18.32
Ocean	1.056±0.011	1.061±0.011	1.069±0.009	1.064±0.008	1.063	91.68	5.39
Dark veg.	1.074±0.004	1.069±0.004	1.091±0.007	1.095±0.006	1.082	164.11	12.41
Bright veg.	1.084±0.005	1.081±0.005	1.117±0.009	1.117±0.007	1.099	196.15	17.54
Dark desert	1.077±0.005	1.072±0.005	1.089±0.005	1.092±0.005	1.083	237.55	18.06
Bright desert	1.078±0.004	1.076±0.003	1.100±0.004	1.101±0.003	1.089	355.91	28.85

The last columns give the average GERB flux $\langle F_g \rangle$ and the difference in average fluxes $\Delta F = \langle F_g \rangle - \langle F_c \rangle$ both in $W m^{-2}$.

and the BARG and HR formats on the other side. The difference of ratio between clearsky and overcast scenes reaches 5.9% for the ARG but is limited to 2.0% and 2.1% for the BARG and the HR. This is explained by the fact that a number of the ARG pixels classified as clear will be contaminated by cloud and vice versa. This contamination is due to the non-correction of the PSF for the ARG, the simple rectification used for the ARG, and the limited accuracy of the GERB geolocation. The net effect is a decrease of m for cloudy scenes and an increase for clearsky scenes. The residual scene type dependency observed in the BARG and HR can be due to the spatial processing but can also be due to imperfect unfiltering of the GERB and/or CERES measurements. The unfiltering error for CERES and GERB is theoretically estimated to less than 1% according to Loeb et al. (2001) and Clerbaux et al. (2008a) respectively. Fig. 2 provides further evidence of scene type dependency affecting the GERB ARG format. On this figure, the GERB/CERES ratio is evaluated in bins of 0.05 of bidirectional reflectance (average of the GERB and CERES reflected radiances divided by the incident Solar irradiance). Unlike the BARG and HR, a significant variation of the GERB/CERES ratio according to the albedo of the scene is observed for the ARG format. This reflectance bin analysis proves that the scene type dependency affecting the ARG in Table 2 is not the result of an issue with the GERB or CERES scene identifications. For instance, it would expect that the ratio will be higher than 1 if the GERB cloud detection fails to detect a significant fraction of the clouds. For the BARG and HR formats, the small decrease of the ratio between the dark and bright scenes is consistent with the 2% difference between clear and cloudy scenes given in Table 2.

Fig. 3 shows the variation of the ratio m according to the Solar Zenith Angle (SZA) and to the Viewing Zenith Angle (VZA) for the 3 GERB formats and for 3 scene types (clear land, clear ocean, and overcast). To get a good sampling of the angles, all the CERES instruments are considered together

for this figure. The ratio m does not exhibit significant dependency on the SZA and VZA except for the clear ocean scene. For this case a significant increase of the ratio m with the VZA is observed. This increase is higher for the ARG than for the BARG and HR formats. As the GERB instrument sensitivity is lower in the blue part of the spectrum, the unfiltering is challenging for clear ocean footprint and higher relative error is expected to occur (Clerbaux et al., 2008a). The importance to have stable GERB/CERES ratio according to the SZA originates from the fact that the comparisons do not cover equally the different condition of illumination, as CERES is on sun-synchronous orbit.

Finally, Fig. 4 shows the regional analysis of the GERB/CERES SW ratio for allsky radiance (first column) and clearsky radiance (second column). Images are given separately for the 4 CERES instruments, as well as their average (FMX). For these images, the GERB radiances have been taken from the BARG format. As expected from the scene type analysis, a slightly lower ratio is observed in areas with frequent cloudiness in the allsky image.

5. Shortwave flux comparison

For the shortwave flux comparison there is no restriction on the angle α and consequently the number of GERB/CERES pairs is much higher than for the radiance comparison. Table 1 shows that this number reaches nearly 2.5 millions per CERES instruments over the 2 months period.

Table 3 summarizes the SW flux comparison in a similar form to that given in Table 2 for the SW radiance. The (BARG) SW flux ratio in all sky conditions lies between 1.066 (FM1 and FM2) and 1.086 (FM4). As for the radiances intercomparison the agreement is better with the FM1 and FM2 than with the FM3 and FM4. All together, the flux ratio is

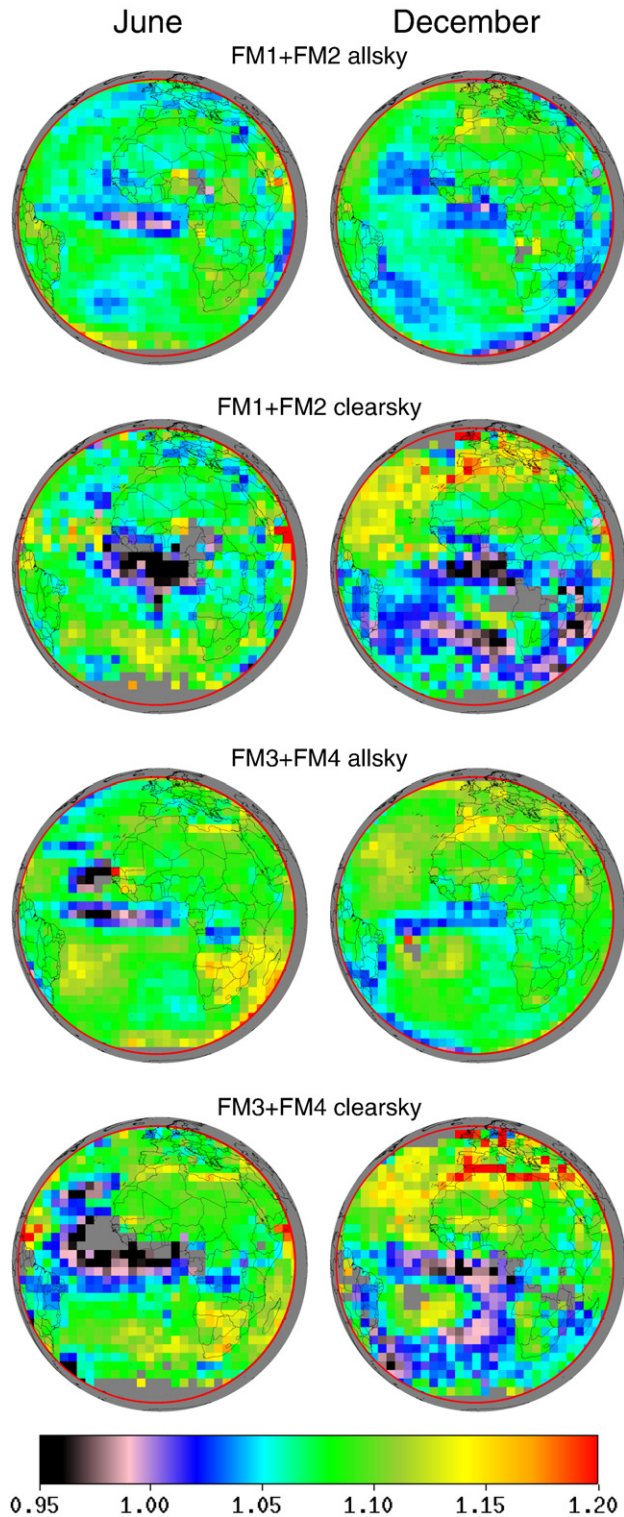


Fig. 5. GERB (BARG)/CERES SW flux ratio for (FM1 + FM2) and (FM3 + FM4) in clearsky and allsky condition. Left panels are for June 2004 and right panels for December 2004.

about 1.5% higher than the ratio observed in radiance. This increase of m between radiance and flux comparisons is higher for the FM1 and FM4 instruments (+2.1% and +1.9%) than for the FM2 and FM3 (+1.2% and +0.9%). This is consistent with the change of sampled area between radiance and flux for the CERES instruments in cross-track scanning. For the FM1 and FM4, the radiances comparisons are in the

tropical region where the ratio is in general slightly lower than the rest of the FOV.

As expected, the SW flux comparison exhibits the same scene type dependency as the radiance comparison: it is largest for the ARG and much more limited for the BARG and HR formats.

Fig. 4 shows the regional analysis of the GERB/CERES SW ratio for allsky and clear sky radiance (1st and 2nd columns) and flux (3rd and 4th columns). Due to the increased number of matches the spatial noise is reduced in the flux comparisons compared to the radiance. Fig. 5 separates the flux comparisons for the June and December periods, for these plots, results from the CERES instruments on the same satellite and therefore sharing the same overpass time have been combined.

Regional patterns are apparent in the flux comparisons which are not visible in the radiance results. As the CERES fluxes are observed from a range of different viewing geometries, errors in the radiance-to-flux conversion, specific to a particular geometry should be minimal in the average quantity used in this comparison, whereas the GERB viewing geometry for each location is fixed. Thus these differences highlight problems in the radiance-to-flux conversions for specific geometries which result in errors in the GERB fluxes for particular locations.

The most obvious feature in the flux plots is a lowering of the ratio off the West coast of Africa. Around the gulf of Guinea this feature is visible in all the flux comparisons, regardless of instrument or season, although it is clearly most pronounced in the clear sky and larger in June than December. Lowered ratios off the African coast at higher and lower latitudes are also seen in some of the plots. To some extent the lowered ratio in the Gulf of Guinea region is present in the radiance comparison, and this could be due to the spectral response characterization in the blue band and the GERB SW radiance unfiltering (Clerbaux et al., 2008a).

However there is clearly an additional issue affecting the fluxes. Considering the region 3°N–3°S and 20°W–2°W, in cloudy conditions the average SW flux ratio, m is 1.061, which is similar to the average overcast value shown in Table 3. However in clear sky the ratio falls to 0.996 that is clearly different from the values seen over most of the rest of the field of view. The ratio for the coangular radiances for clear scenes in this region is 1.022, which although lower than the surrounding regions is clearly not sufficient to explain the flux effect. Although this affected region is subject to significant aerosol contamination, this can be shown not to be the cause of the problem as decomposing the result by aerosol loading using the aerosol parameters present in the CERES SSF files indicates that the disagreement is actually reduced in the presence of aerosol.

However considering the ratio in the region as a function of sun-glint angle shows that the low GERB/CERES SW flux ratio occur when the GERB direction of observation is close to the sun specular reflection. To explain this it must be understood what happens to the GERB fluxes for clear ocean scenes in the region of the glint angle. For glint angles between 0 and 15°, no GERB flux is produced in the Edition 1 and V003 products, due to the problem of obtaining an accurate scene identification. For glint angles between 15 and 25° the GERB radiance is not used as the basis of the flux due to the problem of determining an accurate anisotropy factor for these angles. In these cases a climatological value of the flux from the CERES TRMM ADM is used. Thus for these angles a comparison is actually being made between a CERES based climatology and a CERES instantaneous estimate and thus it is not surprising that the ratio is close to 1. As the glint angle varies with time of day and season the location of the lowered ratios varies according to which CERES instrument (i.e. overpass time) and in which season the comparison is made.

A much more localised, but nevertheless persistent difference is observed in the form of elevated flux ratios some (small) regions of the desert on the African continent and in Spain. These are most obvious in the clear sky flux comparisons and more apparent in the December

Table 4
GERB/CERES LW radiance ratio m and uncertainty for $\alpha < 5^\circ$

Scene type	FM1	FM2	FM3	FM4	<FM>	<L _g >	ΔL
<i>Averaged Rectified Geolocated (ARG)</i>							
Allsky	0.989±0.001	0.993±0.001	0.983±0.001	0.981±0.001	0.986	84.22	-1.17
June	0.989±0.001	0.993±0.001	0.984±0.001	0.982±0.001	0.987	86.64	-1.14
December	0.989±0.001	0.993±0.001	0.981±0.001	0.980±0.001	0.986	81.90	-1.20
Day	0.994±0.001	0.994±0.001	0.983±0.001	0.981±0.001	0.988	85.80	-1.05
Night	0.983±0.001	0.989±0.002	0.982±0.001	0.981±0.002	0.984	82.23	-1.34
Clearsky	0.983±0.001	0.995±0.001	0.982±0.001	0.980±0.001	0.985	95.44	-1.45
Cloudy	1.015±0.005	0.998±0.003	0.998±0.006	0.999±0.005	1.002	67.26	0.14
<i>Binned Averaged Rectified Geolocated (BARG)</i>							
Allsky	0.989±0.001	0.993±0.001	0.983±0.001	0.981±0.001	0.987	84.15	-1.15
June	0.989±0.001	0.993±0.001	0.984±0.001	0.983±0.001	0.987	86.46	-1.12
December	0.989±0.001	0.993±0.001	0.981±0.001	0.980±0.001	0.986	81.94	-1.18
Day	0.995±0.001	0.994±0.001	0.983±0.001	0.981±0.001	0.988	85.71	-1.04
Night	0.983±0.001	0.989±0.001	0.983±0.001	0.982±0.001	0.984	82.22	-1.30
Clearsky	0.986±0.001	0.997±0.001	0.984±0.001	0.984±0.001	0.988	95.52	-1.19
Cloudy	0.991±0.003	0.983±0.002	0.982±0.002	0.978±0.003	0.983	65.73	-1.11
<i>High Resolution (HR)</i>							
Allsky	0.989±0.001	0.993±0.001	0.983±0.001	0.982±0.001	0.987	84.93	-1.15
June	0.990±0.001	0.993±0.001	0.984±0.001	0.983±0.001	0.987	87.00	-1.11
December	0.989±0.001	0.993±0.001	0.982±0.001	0.980±0.001	0.986	82.95	-1.18
Day	0.995±0.001	0.993±0.001	0.983±0.001	0.981±0.001	0.988	86.57	-1.05
Night	0.984±0.001	0.990±0.001	0.983±0.001	0.982±0.001	0.985	83.10	-1.29
Clearsky	0.987±0.001	0.998±0.001	0.985±0.001	0.984±0.001	0.988	95.78	-1.12
Cloudy	0.988±0.002	0.980±0.002	0.977±0.001	0.976±0.002	0.981	68.28	-1.35

The last columns give the average GERB radiance $\langle L_g \rangle$ and the difference in average radiance $\Delta L = \langle L_g \rangle - \langle L_c \rangle$ both in $W\ m^{-2}\ sr^{-1}$.

comparisons than in the June results. These differences relate to a known problem with the radiance-to-flux conversion for these scenes and improved angular dependency models for semi-desert regions are planned (Bertrand et al., submitted for publication).

6. Longwave radiance comparison

Table 4 displays the GERB/CERES LW radiance comparison results. In contrast with the SW, the GERB LW radiance is generally lower than

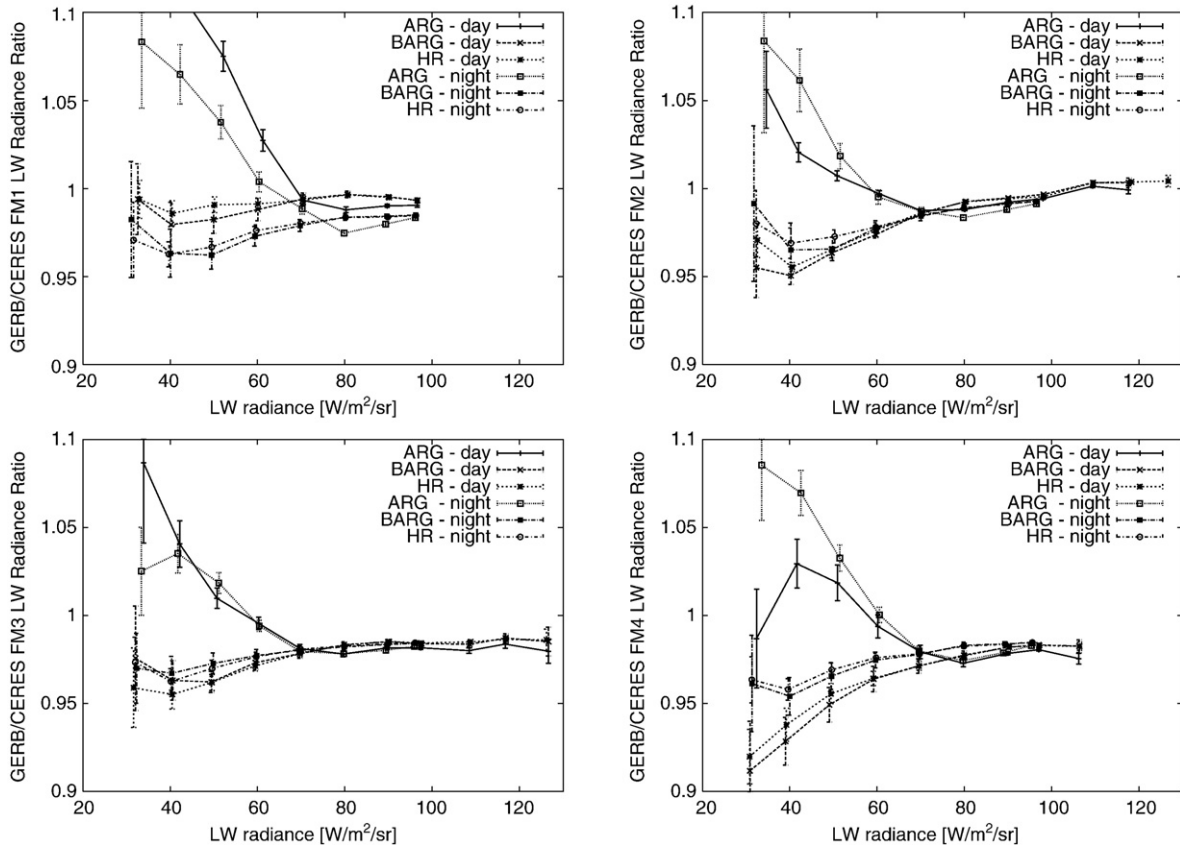


Fig. 6. GERB/CERES LW radiance ratio in radiance bins.

CERES. The GERB/CERES longwave radiance ratio m differs significantly between the 4 CERES instruments and lies between $m=0.981$ (FM4) and $m=0.993$ (FM2). In addition to the average allsky ratio, the results are shown separately for June and December, for day ($SZA < 85^\circ$) and night ($SZA > 95^\circ$) conditions, and for clear and cloudy scenes.

For cloudy scenes, the GERB/CERES ratio is slightly higher for the ARG than for the BARG and HR formats. The explanation for this is the same as for the SW radiance comparison over clear ocean, except that here the cloudy scenes have the lower radiances. Fig. 6 shows the dependency of the ratio with the LW radiance. In addition to the scene type dependency affecting the ARG format for very cold scenes, a significant day/night difference is observed with the FM1 (1.1%) and to a lesser extent with the FM2 (0.5%). As the problem is not present with the FM3 and FM4, it is assumed to be due to the LW separation

for the CERES instruments on Terra. For the BARG and HR formats the GERB/CERES ratio is lower for cold (i.e. cloudy) scenes than for warm (i.e. clear) scenes. Theoretical studies show that the CERES LW radiances are expected to be slightly overestimated for cloudy scenes. Loeb et al. (2001) have shown that although the CERES LW unfiltering error remains in general below 0.2% it can reach 0.4% for deep convective clouds (overestimation). On the other hand, the GERB unfiltering is expected to slightly underestimate the radiance for cloudy scenes (Clerbaux et al., 2008b). The cumulative effect of these 2 error sources explains the observed drop in ratio for the coldest scenes in Fig. 6 for the BARG and HR.

The first and second columns in Fig. 7 show the radiance ratio in allsky and clearsky conditions. For the FM2 instrument, slightly higher LW radiance ratio is observed over warm desert. This corresponds to

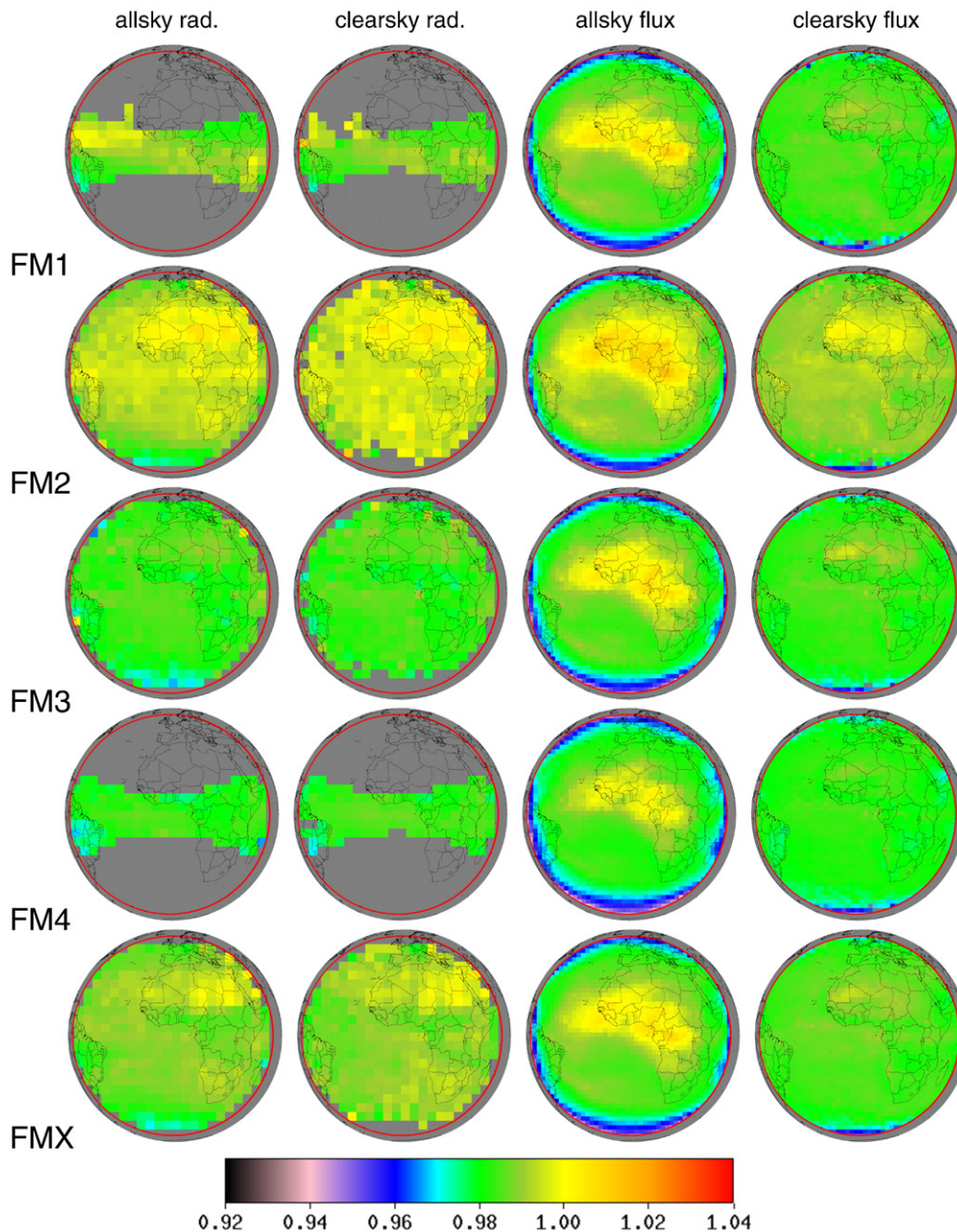


Fig. 7. GERB (BARG)/CERES LW ratio for the different CERES instruments and all together (FMX). The red circle indicates $VZA = 70^\circ$.

Table 5
GERB/CERES LW flux ratio m and uncertainty

Scene type	FM1	FM2	FM3	FM4	<FM>	<F _g >	ΔF
<i>Averaged Rectified Geolocated (ARG)</i>							
Allsky	0.988±0.001	0.992±0.001	0.986±0.001	0.983±0.001	0.987	257.35	-3.28
June	0.987±0.001	0.992±0.001	0.987±0.001	0.984±0.001	0.988	263.96	-3.34
December	0.989±0.001	0.992±0.001	0.986±0.001	0.982±0.001	0.987	250.94	-3.22
Day	0.992±0.001	0.994±0.001	0.988±0.001	0.983±0.001	0.989	262.63	-2.86
Night	0.983±0.001	0.990±0.001	0.985±0.001	0.984±0.001	0.986	251.87	-3.71
Clearsky	0.982±0.001	0.990±0.001	0.982±0.001	0.979±0.001	0.983	291.98	-4.99
Cloudy	1.003±0.001	1.001±0.001	1.000±0.002	0.995±0.001	1.000	204.56	-0.01
<i>Binned Averaged Rectified Geolocated (BARG)</i>							
Allsky	0.988±0.001	0.992±0.001	0.987±0.001	0.983±0.001	0.987	257.20	-3.26
June	0.987±0.001	0.992±0.001	0.987±0.001	0.984±0.001	0.987	263.76	-3.35
December	0.989±0.001	0.992±0.001	0.986±0.001	0.983±0.001	0.987	250.83	-3.18
Day	0.992±0.001	0.994±0.001	0.988±0.001	0.983±0.001	0.989	262.56	-2.85
Night	0.983±0.001	0.990±0.001	0.985±0.001	0.984±0.001	0.986	251.89	-3.67
Clearsky	0.984±0.001	0.991±0.001	0.984±0.001	0.981±0.001	0.985	292.12	-4.51
Cloudy	0.991±0.001	0.990±0.001	0.989±0.002	0.983±0.002	0.988	202.02	-2.38
<i>High Resolution (HR)</i>							
Allsky	0.985±0.001	0.989±0.001	0.983±0.001	0.981±0.001	0.984	255.37	-4.03
June	0.984±0.001	0.989±0.001	0.984±0.001	0.982±0.001	0.985	262.42	-4.03
December	0.985±0.001	0.989±0.001	0.982±0.001	0.980±0.001	0.984	248.52	-4.04
Day	0.989±0.001	0.991±0.001	0.984±0.001	0.980±0.001	0.986	260.51	-3.71
Night	0.981±0.001	0.987±0.001	0.982±0.001	0.981±0.001	0.983	250.27	-4.37
Clearsky	0.981±0.001	0.989±0.001	0.981±0.001	0.979±0.001	0.983	290.66	-5.15
Cloudy	0.985±0.001	0.983±0.001	0.981±0.001	0.978±0.001	0.982	205.39	-3.85

The last columns give the average GERB flux <F_g> and the difference in average flux ΔF = <F_g> - <F_c> both in W m⁻².

the increase of the ratio m seen for the FM2 for warm scenes (see upper right graph of Fig. 6).

7. Longwave flux comparison

Table 5 reports the LW flux intercomparisons in a similar form to Table 4. The GERB/CERES flux ratio in all sky conditions lies between $m=0.983$ (FM4) and $m=0.992$ (FM2). The average across the 4 CERES instruments is $m=0.987$ which is in agreement with the radiance comparison. As for the shortwave, the agreement is better with the FM1 and FM2 than with the FM3 and FM4 (Fig. 8). All together, the GERB LW flux appears to be about 1.3% lower than CERES ($m=0.987$).

As for all the previous comparisons, the difference between the clear and cloudy ratios is higher for the ARG (1.7%) than for the BARG (0.3%) and HR (0.1%) formats.

The third and fourth columns in Fig. 7 show the flux ratio in allsky and clearsky conditions respectively. In clearsky conditions there is no obvious problem affecting the GERB fluxes at the regional scale, at least for GERB VZA lower than 70° (red circle). On the other hand, the allsky plot (left) gives further evidence of GERB LW flux error over cloudy scenes. This problem was already reported by Dewitte et al. (2008). The GERB LW radiance-to-flux conversion (Clerbaux et al., 2003a) does not fully compensate for the limb-darkening associated with high clouds. Similar radiance-to-flux conversion error is suspected in case of aerosol (Ali Bahmal, pers. comm.). This is the cause of the high ratio observed for viewing angles close to nadir (center of the disk) and the lower ratio on the borders of the disk. As expected, the lowest errors are associated with viewing zenith angles close to VZA ~ 52° due to the near independence of the scene type and the flux/radiance ratio around this angle (Otterman et al., 1997).

Although the observation angle is favorable (VZA ~ 55°) an increase of the GERB/CERES ratio is observed over the Alps in clearsky conditions. Compared to the surrounding area there is a local increase of the LW flux ratio of about 1%. This is an effect of azimuthal anisotropy which is not taken into account in the GERB LW radiance-to-flux conversion. Due to its geostationary orbit the GERB instrument mainly measures radiance emitted by the south faces of the mountains in the Northern hemisphere (and the opposite in the Southern hemisphere).

This could introduce small bias as south faces present higher temperature than north faces (Clerbaux et al., 2003b).

8. Summary

The GERB-2 ARG, BARG and HR and CERES SSF Edition-2/Rev1 FM-1,-2,-3,-4 TOA radiative products have been compared for 2 months in 2004. Detailed results of the comparisons of shortwave radiance, shortwave flux, longwave radiance and longwave flux have been presented.

In the shortwave, the GERB radiance and flux are respectively about 5.9% and 7.5% higher than CERES (averaged over the 4 CERES instruments). Except for the ARG products, scene type dependency of the GERB/CERES ratio is limited to about 1% around these mean values. Therefore a difference in the absolute calibration of the GERB and CERES SW channels seems the most likely cause of the discrepancy. The observed ratio of 1.059 ± 0.004 for the SW radiance seems to agree with the arithmetic sum of the 95% confidence levels (2 SD) of both GERB (3.8%) and CERES (2%). However, as the calibrations and data processing of the instruments have been kept totally independent, the uncertainty on the difference is the RMS of the uncertainties, thus 4.3% at the 95% confidence level. Assuming normal distributions with the SD given before, the probability that the ratio of one instrument on the other reaches a value of 1.055 is only 1.4%. It is therefore likely that the absolute accuracy of one or both instruments is poorer than theoretically expected in the SW.

The results presented here highlight the differences between the GERB products. In particular they show the difficulty of using GERB ARG data to isolate the effect of small regions or individual scene types and the errors associated with not considering the full extent and detail of the instrument PSF. The GERB BARG and HR formats are easier to compare with other instruments and display more consistent differences with CERES for the comparisons shown here. These formats are in the process of being validated and officially released for scientific use by the GERB team.

In the longwave, GERB is 1.3% lower than CERES for both the radiance and the flux. This is consistent with the combined stated 1 SD accuracies of 0.75% for CERES and 0.9% for GERB (the combined RMS is

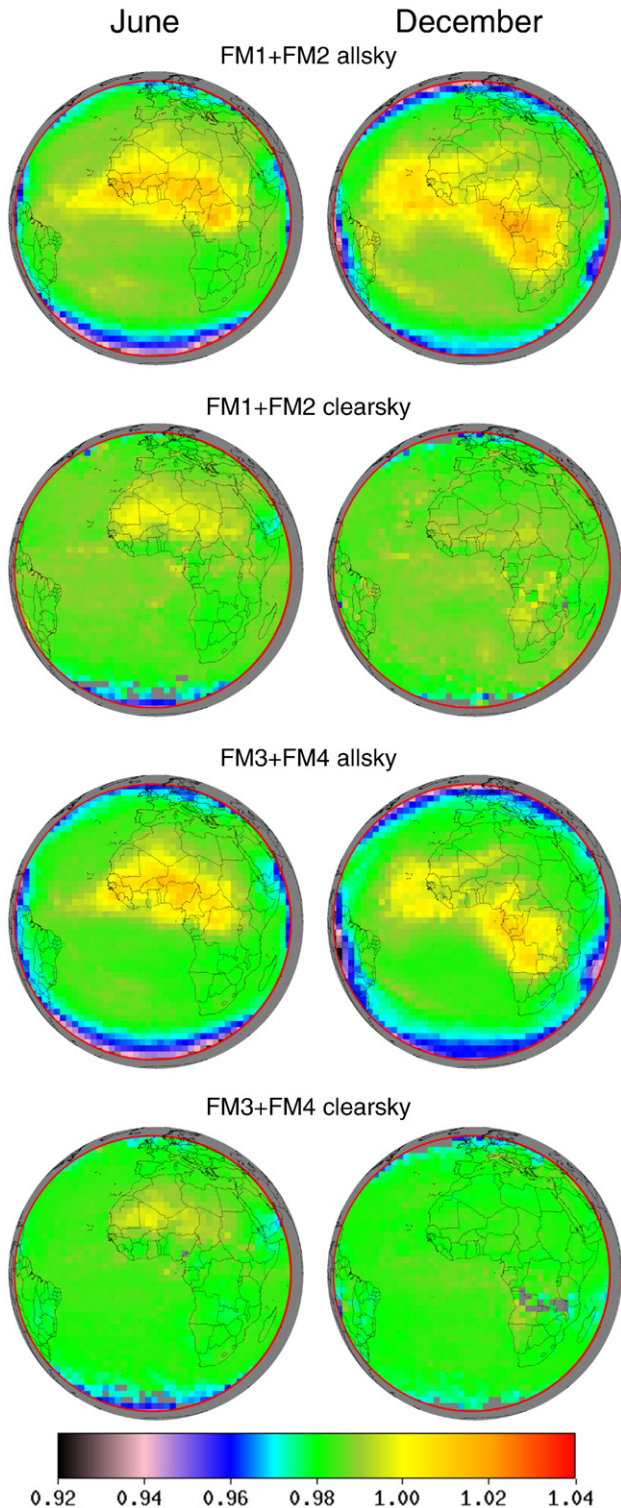


Fig. 8. GERB (BARG)/CERES LW flux ratio for (FM1+FM2) and (FM3+FM4) in clearsky and allsky condition. Left panels are for June 2004 and right panels for December 2004.

1.2%). The GERB LW radiance-to-flux conversion performs correctly for clear scenes but does not totally compensate for the anisotropy for some cloudy scenes. A residual longwave flux limb-darkening is observed in cloudy and in allsky conditions. Preliminary investigations showed that this problem could be corrected in GERB Edition-2 by better treatment of the anisotropy for high semi-transparent clouds (cirrus).

Acknowledgements

The authors are grateful to the Atmospheric Sciences Data Center at NASA Langley Research Center for providing the CERES data used in this work.

References

- Bertrand, C., Ipe, A., Clerbaux, N., & Gonzalez, L. (submitted for publication). GERB SW flux anomalies over the sahel region: An ADM related issue. *Advances in Space Research*.
- Clerbaux, N., Bertrand, C., Caprion, D., Depaeppe, B., Dewitte, S., Gonzalez, L., et al. (2005). Narrowband-to-broadband conversions for SEVIRI. *Proc. of the 2005 EUMETSAT meteorological satellite conference*, P46 (pp. 351–357). Available online from <http://www.eumetsat.int>
- Clerbaux, N., Dewitte, S., Bertrand, C., Caprion, D., Depaeppe, B., Gonzalez, L., et al. (2008). Unfiltering of the Geostationary Earth Radiation Budget (GERB) data. Part I: Shortwave radiation. *Journal of Atmospheric and Oceanic Technology*, 25(7), 1087–1105.
- Clerbaux, N., Dewitte, S., Bertrand, C., Caprion, D., Depaeppe, B., Gonzalez, L., et al. (2008). Unfiltering of the Geostationary Earth Radiation Budget (GERB) data. Part II: Longwave radiation. *Journal of Atmospheric and Oceanic Technology*, 25(7), 1106–1117.
- Clerbaux, N., Dewitte, S., Gonzalez, L., Bertand, C., Nicula, B., & Ipe, A. (2003). Outgoing longwave flux estimation: Improvement of angular modelling using spectral information. *Remote Sensing of Environment*, 85, 389–395.
- Clerbaux, N., Ipe, A., Bertand, C., Dewitte, S., Nicula, B., & Gonzalez, L. (2003). Evidence of azimuthal anisotropy for the thermal infrared radiation leaving the Earth's atmosphere. *International Journal of Remote Sensing*, 24, 3005–3010.
- Dewitte, S., Gonzalez, L., Clerbaux, N., Ipe, A., & Bertrand, C. (2008). The geostationary earth radiation budget Edition 1 data processing algorithms. *Advances in Space Research*, 41(1), 906–913.
- Haefelin, M., Wielicki, B., Duval, J. P., Priestley, K., & Viollier, M. (2001). Inter-calibration of CERES and ScaRaB Earth radiation budget datasets using temporally and spatially collocated radiance measurements. *Geophys. Res. Lett.*, 28, 167–170.
- Harries, J., Russell, J., Hanafin, J., Brindley, H., Futyran, J., Rufus, J., et al. (2005). The geostationary earth radiation budget project. *Bulletin of the American Meteorological Society*, 86(7), 945–960.
- Ipe, A., Bertrand, C., Clerbaux, N., Dewitte, S., & Gonzalez, L. (submitted for publication). The GERB Edition 1 products SEVIRI scene identification — Part I: Methodology. *IEEE Transactions on Geoscience and Remote Sensing*.
- Loeb, N. G., Kato, S., & Wielicki, B. A. (2002). Defining top-of-the-atmosphere flux reference level for Earth radiation budget studies. *Journal of Climate*, 15, 3301–3309.
- Loeb, N. G., Priestley, K., Kratz, D., Geier, E., Green, R., Wielicki, B., et al. (2001). Determination of unfiltered radiances from the clouds and the earth's radiant energy system instrument. *Journal of Applied Meteorology*, 40, 822–835.
- Loeb, N. G., Wielicki, B. A., Doelling, D. R., Smith, G. L., Kayes, D. F., Kato, S., et al. (in press). Towards optimal closure of the Earth's top-of-atmosphere radiation budget. *Journal of Climate*.
- Otterman, J., Starr, D., Brakke, T., Davies, R., Jacobowitz, H., Mehta, A., et al. (1997). Modeling zenith-angle dependence of outgoing longwave radiation: Implication for flux measurements. *Remote Sensing of Environment*, 62, 90–100.
- Russell, J. (2006). *Quality summary for GERB Edition-1 L2 ARG*. Reference document: 2006 : Imperial College.
- Schmetz, J., Pili, P., Tjemkes, S., Just, D., Kerkmann, J., Rota, S., et al. (2002). An introduction to Meteosat Second Generation (MSG). *Bulletin of the American Meteorological Society*, 83, 977–992.
- Smith, G. L., Szewczyk, Z. P., Mlynczak, P. E., Lee, R. B., III, Wielicki, B. A., Priestley, K. J., et al. (2003). Method for comparison of GERB and CERES radiances. *Proc. 10th int. symp. remote sensing, Spain, Soc. Photo-Optical Instrumentation Engineers* (pp. 5234).
- Wielicki, B. A., Barkstrom, B. R., Harrison, E. F., Lee, R. B., III, Smith, G. L., & Cooper, J. E. (1996). Clouds and the Earth's Radiant Energy System (CERES): An earth observing system experiment. *Bulletin of the American Meteorological Society*, 77, 853–868.